Exposure of Phosphatidylinositol Transfer Proteins to Sphingomyelin−Cholesterol Membranes Suggests Transient but Productive Interactions with Raft-Like, Liquid-Ordered Domains[†]

Elizabeth C. Miller and George M. Helmkamp, Jr.*

Department of Biochemistry and Molecular Biology, Mail Stop 3030, University of Kansas Medical Center, 3901 Rainbow Boulevard, Kansas City, Kansas 66160-7421

Received April 17, 2003; Revised Manuscript Received September 22, 2003

ABSTRACT: Both isoforms of rat phosphatidylinositol transfer protein (PITP) mediate the intermembrane transfer of sphingomyelin (Cer*P*Cho). In the plasma membrane, Cer*P*Cho often segregates with cholesterol into microdomains such as lipid rafts and caveolae. To test the hypothesis that PITP exhibits a preference for Cer*P*Cho- and cholesterol-rich membranes, we prepared unilamellar vesicles containing variable amounts of these two lipids. We also used Cer*P*Cho species with different acyl composition and treated vesicles with agents known to sequester and remove cholesterol. We observed that the β isoform of rat PITP was more sensitive to membrane cholesterol than was the α isoform, as shown by increases in specific activities of lipid transfer of 2−6-fold. A relatively high membrane content of cholesterol (mole fraction > 0.4) was required to elicit such enhancements. Treatment of cholesterol-rich membranes with a series of β cyclodextrins demonstrated that, upon depletion of cholesterol from participating membranes, the PITPβ activity changes were fully reversible. We finally noted that the mechanism by which cholesterol enhances the activity of PITPβ appeared to involve a decreased affinity of the protein for the membrane surface, in a manner that was independent of vesicle size and membrane microviscosity. We conclude that PITPβ interacts transiently but productively with the liquid-ordered phase formed by Cer*P*Cho and cholesterol and discuss the possibility of PITP interactions in vivo with sphingolipid- and cholesterol-rich membrane microdomains.

Testing the hypothesis that cytosolic proteins were required to transport cellular phospholipids from membranes in which they were synthesized to those in which they functioned (*1*), phospholipid transfer proteins were isolated and characterized from several mammalian tissues (*2*−*4*). Designated by the lipid for which they have the greatest preference (e.g., phosphatidylinositol (PtdIns)[1] or PtdCho, respectively), PITP and PCTP have recently emerged as two members of a protein family that share the unique START domain (*5*−*8*). To date, sequence homologies have identified nearly 40 PITP-like proteins, mostly in metazoans (*9*). In mammals, two soluble isoforms are commonly expressed: PITPα and PITPβ share nearly 80% sequence identity but exhibit subtle differences in subcellular location (*10*) and substrate specificity (*11*, *12*).

The distinguishing feature of the START domain is an amphipathic lipid-binding cavity formed between a highly curved β sheet and a number of short or long α helices (*13*). This cavity effectively and completely sequesters one molecule of phospholipid from the external aqueous environment, as evidenced by X-ray crystallographic studies of the membrane-free, liganded structures of PITP and PCTP (*6*, *8*). However, the mechanism by which the cavity opens and closes in the membrane-bound state to permit lipid exchange with the membrane remains to be elucidated. Indeed, it is this membrane-bound intermediate that is most likely essential not only to intermembrane phospholipid transport in general but to more specialized participation in signal transduction, vesicle trafficking, and cellular lipid metabolism (*6*, *14*−*17*).

Cellular functions of PITPs, both documented and proposed, suggest that interactions with the plasma membrane are highly probable. We and others have recently demonstrated that both isoforms of mammalian PITP can bind and transport Cer*P*Cho, albeit at rates markedly lower than those for PtdIns and PtdCho (*11*, *12*). Moreover, PITPβ possesses a higher activity toward Cer*P*Cho than PITPα. Sphingolipids, including Cer*P*Cho and glycosphingolipids, represent a small but essential class of lipids in all eukaryotic cells (*18*). They are vital to cell development and differentiation, signal transduction, protein sorting, and through their physical-chemical properties, spatial organization within membranes (*19*). The fraction of Cer*P*Cho on the cytosolic surface of cellular membranes and potentially accessible to PITP is, however, limited (*20*). Cer*P*Cho is often localized with

[†] This research was supported by grant GM59162 from the National Institutes of Health.

* To whom correspondence should be addressed. Tel: (913) 588-6958. Fax: (913) 588-7440. E-mail: ghelmkam@kumc.edu.

[1] Abbreviations: CD, cyclodextrin; Cer*P*Cho, sphingomyelin; DPH, 1,6-diphenyl-1,3,5-hexatriene; LacCer, lactosylceramide; LacPtdEtn, *N*-lactosylphosphatidylethanolamine; PCTP, phosphatidylcholine transfer protein; PITP, phosphatidylinositol transfer protein; PtdCho, phosphatidylcholine; PtdIns, phosphatidylinositol; PtdOH, phosphatidate; χ, mole fraction; 14:0-Cer*P*Cho, *N*-myristoyl-sphingomyelin; 18:1(9)-Cer*P*Cho, *N*-oleoyl-sphingomyelin.

10.1021/bi034616n CCC: $25.00
Published on Web 10/24/2003

glycosphingolipids and cholesterol in the well-characterized plasma membrane microdomains known as rafts and caveolae (*21*−*23*). Cer*P*Cho and cholesterol appear to follow a gradient of progressive enrichment along the classical secretory pathway, culminating in levels exceeding 50% or more of their total cell content in the (apical) plasma membrane (*24*, *25*). Observations of the cosegregation of Cer*P*Cho and cholesterol in lipid mixtures and during membrane biogenesis find an explanation in the physical-chemical properties of these two lipids (*26*).

We have undertaken the current study to investigate in detail the ability of PITPβ to transport Cer*P*Cho and to interact with small unilamellar vesicles containing this lipid as its bulk constituent. We further examine the influence of membrane cholesterol content on some of the physical properties of these vesicles and their efficiency in protein-mediated transfer of Cer*P*Cho and glycerophospholipids. We present data that show enhanced lipid transport to Cer*P*Cho vesicles that contain significant amounts of cholesterol and that this effect can be abrogated in the presence of agents that complex with cholesterol. We also demonstrate that the improved environment for protein-mediated lipid transport is independent of changes in vesicle size or membrane microviscosity. Finally, we discuss the possibility of PITP interactions in vivo with sphingolipid- and cholesterol-rich membrane microdomains.

MATERIALS AND METHODS

Materials. Chicken egg yolk PtdCho, 1,2-dioleoyl-PtdOH, porcine liver PtdIns, *N*-lactosyl-1,2-dioleoyl-PtdEtn, *N*-oleoyl-Cer*P*Cho, porcine brain Cer*P*Cho, chicken egg yolk Cer*P*Cho, and cholesterol were purchased from Avanti Polar Lipids (Alabaster, AL). *N*-Myristoyl-Cer*P*Cho was a generous gift from R. E. Brown (Austin, MN). Cholesteryl oleate, dihydrocholesterol, β cyclodextrin, methyl-β cyclodextrin, filipin III, and glycogen (rabbit liver, type III) were obtained from Sigma (St. Louis, MO). 2-Hydroxypropyl-β cyclodextrin was supplied by Cyclodextrin Technologies Development (High Springs, FL). Purchased from PerkinElmer Life Sciences (Boston, MA) were [9,10-^{3}H]oleic acid (310 Gbq mmol^{-1}), [1-^{14}C-*oleoyl*]cholesteryl oleate (2.1 Gbq mmol^{-1}), [1-^{14}C-*oleoyl*]1-palmitoyl-2-oleoyl-PtdCho (1.9 Gbq mmol^{-1}), [2-^{3}H-*inositol*]PtdIns (407 Gbq mmol^{-1}), and from Amersham Biosciences (Piscataway, NJ), bovine brain [*N*-^{14}C-*methyl*]Cer*P*Cho (2.1 Gbq mmol^{-1}). Cholesteryl [9,10-^{3}H]oleate was synthesized according to published procedures (*27*). All lipids were >95% pure when analyzed by thin-layer chromatography. 1,6-Diphenyl-1,3,5-hexatriene was supplied by Molecular Probes (Eugene, OR). A cDNA encoding rat PITPα was generated in our laboratory (*28*); another encoding rat PITPβ was kindly donated by K. Hosaka (Maebashi, Japan). RCA-120 agglutinin was isolated from castor beans (*Ricinus communis*) according to a published protocol (*29*). Other chemicals were reagent-grade and the highest purity available.

Expression of Recombinant PITPα and PITPβ. The cDNAs encoding unmodified, full-length forms of rat PITPα and rat PITPβ were introduced into the pET-11c vector. Following transformation of an *Escherichia coli* BL21(DE3) host in which two molecular chaperones (*dna*K and *gro*ELS) were coexpressed (*30*), proteins were expressed in cells grown at 20 °C. Purification from cell-free lysates employed molecular sieve (Sephadex G-100, Amersham), anion exchange (Q Sepharose Fast Flow, Amersham), and hydroxylapatite (Bio-Rad HP, BioRad Laboratories, Hercules, CA) chromatography. Concentrations of recombinant rat PITPα and rat PITPβ proteins were based on ϵ_M values of 79 700 and 74 500 M^{-1} cm^{-1} at 279 nm, respectively (*31*).

Intermembrane Lipid Transfer Activity. Lipid transfer activity of PITPs was determined by measuring the rate of radiolabeled phospholipid from donor to acceptor vesicles, as described (*32*). Small unilamellar vesicles were prepared by sonication and centrifugation or by rapid injection of ethanol/dimethyl sulfoxide (80:20, vol %) solutions. Prior to use, vesicles were passed through a polyvinylidene fluoride filter (0.45 μm pore, Millex, Millipore, Fisher Scientific, Pittsburgh, PA). In most cases, the bulk membrane lipid was egg PtdCho, liver PtdCho, or brain Cer*P*Cho; transfer substrates include [^{3}H-*oleoyl*]PtdCho or [^{14}C-*choline*]Cer-*P*Cho. Donor vesicles contained 10 mol % LacPtdEtn; acceptor vesicles were prepared with a trace amount of either cholesteryl [^{3}H]oleate or cholesteryl [^{14}C]oleate as an internal standard in the double-isotope analysis of vesicle recovery and extent of phospholipid transfer. The buffer employed in the assays was 10 mM HEPES-Na, 50 mM NaCl, and 1 mM Na_2EDTA (pH 7.4). All vesicle amounts and concentrations reflected the phospholipid components and were based upon lipid phosphorus determination following chloroform/methanol (50:50, vol %) extraction of suitable aliquots. The component of cholesterol, when present, was expressed as the mole fraction (χ) of the total vesicle lipid. Assays, unless otherwise specified, were performed at 37 °C for 30 min; controls were carried out in the absence of PITP. Separation of vesicle populations was achieved by agglutination and precipitation of donor membranes in the presence of *R. communis* agglutinin (*32*). Acceptor vesicle recovery was 85−95%; contamination by donor vesicles was <10%. Care was taken to ensure that assays were performed under conditions in which the rate of transfer was directly proportional to the amount of PITP present. We have long recognized that multiple transfer pathways are possible within our assay system of two distinct vesicle populations (*33*) but have designed our experimental conditions to monitor just one, namely, donor to acceptor. Moreover, we assume, for calculations of transfer activity, that the small amount of radiolabeled phospholipid initially present in the donor vesicle and later recovered in the acceptor vesicle reflects the bulk pool of that phospholipid. That this assumption is valid is supported by several studies that indicate rather broad flexibility in the binding and transfer by PITPs of lipid substrates with a different acyl chain composition (*6*, *34*, *35*).

Analysis of Vesicle Size. The mean particle size and polydispersity of vesicle preparations were determined by dynamic light scattering using a DynaPro-LSR instrument (Protein Solutions, Charlottesville, VA). Vesicle preparations were diluted to a concentration of 50 μM and centrifuged at 14 000*g* for 30 min immediately before measurements were taken. Regularization intensity data were obtained at 20 °C, and monomodal cumulants were analyzed to provide hydrodynamic radius values.

Fluorescence Anisotropy Measurements. Unilamellar vesicles were prepared by solvent injection, followed by brief

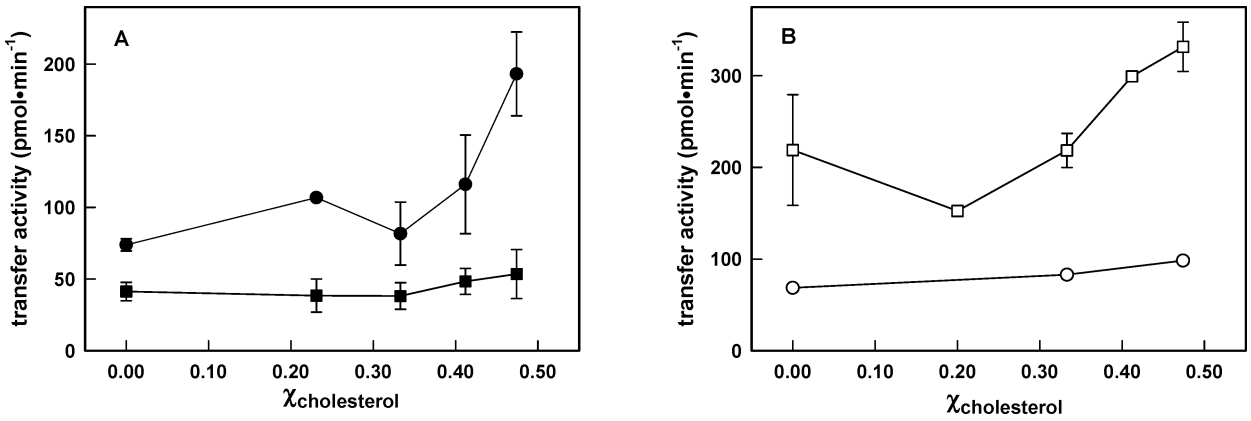

FIGURE 1: Effect of acceptor vesicle cholesterol content on phospholipid transfer. (A) Acceptor vesicles were prepared from brain Cer*P*Cho and PtdOH (98:2, mol %) and the indicated mole fraction of cholesterol. Using donor vesicles prepared from brain Cer*P*Cho, PtdOH, and LacPtdEtn (88:2:10, mol %), assays of Cer*P*Cho transfer were performed with 2 μg of PITPα (■) or PITPβ (●), with data presented as the mean ± SD of three to six determinations. (B) Acceptor vesicles were prepared from egg PtdCho and PtdOH (98:2, mol %) and the indicated mole fraction of cholesterol. Using donor vesicles prepared from egg PtdCho, PtdOH, and LacPtdEtn (88:2:10, mol %), assays of PtdCho transfer were performed with 0.1 μg of PITPα (□) or PITPβ (○), with data presented as the mean ± SD of three to six determinations.

probe sonication and centrifugation. DPH was added from a stock solution of 1 mM in *N*,*N*-dimethylformamide to achieve a lipid-to-probe ratio between 500 and 750. Vesicles (0.5 mM) were then incubated in the dark at 37 °C for 1 h to allow complete equilibration. Steady-state anisotropy measurements were made with a Pi-Star180 spectrometer (Applied Photophysics, Leatherhead, UK), equipped with an equilibrium sample handling unit, thermostated cell holder, and a 400 nm long-pass cutoff filter (Melles-Griot, Irvine, CA) in front of the emission photomultiplier tube. Excitation wavelength was set at 357 nm; slit widths were fixed at 1 nm; excitation and emission path lengths were 1.0 and 0.4 cm, respectively. A 10 mg mL^{-1} solution of glycogen in water was used for instrument calibration. Inner filter effects were minimized by adjusting sample absorption (357 nm) values to <0.13. Correlation between DPH steady-state fluorescence anisotropy and the viscosity of fluid media has been discussed (*36*).

Application of Cholesterol-Binding Agents. β-CDs, synthetic cyclic oligosaccharides, and filipin III, a fungal polyene macrolide, were prepared as stock solutions in buffer and ethanol, respectively, and added to the assay mixture containing all reactants except transfer protein, unless otherwise specified. After an incubation at 37 °C for various times, PITPα or PITPβ was added, and the assay continued. Appropriate controls were carried out to ensure that the levels of agent used did not interfere with vesicle recovery or spontaneous phospholipid transfer.

Binding of PITPβ to Phospholipid Vesicles. Vesicles were prepared from Cer*P*Cho and PtdOH (98:2, mol %), and when indicated, cholesterol (χ = 0.47). PITPβ (20 μg) was incubated in 300 μL of assay buffer in the absence or presence of 0.75 mM vesicles at 37 °C for 30 min. From these mixtures, 250 μL aliquots were analyzed by HPLC, using a TosoHaas G2000SW molecular sieve column eluted with assay buffer at a flow rate of 1 mL min^{-1}, as previously described (*37*). The instrumentation was a LC-6A system (Shimadzu, Columbia, MD) controlled by Class-VP software. Protein was monitored by ultraviolet absorbance at 275 nm and intrinsic Trp fluorescence, using λ_{ex} of 290 nm and λ_{em} of 340 nm.

RESULTS

Effect of Vesicle Cholesterol Content and Location on Phospholipid Transfer. We investigated the effect of cholesterol added to one or both of the membrane populations employed in phospholipid transfer assays. When Cer*P*Cho was the bulk lipid as well as the transferred lipid, we observed a dramatic increase in transfer activity for PITPβ (Figure 1A) when cholesterol was included in the vesicle lipid compositions, up to χ = 0.47. Under these same conditions, there was no change in the transport of Cer*P*Cho by PITPα. Opposite results were seen when PtdCho was the bulk and transferred lipid (Figure 1B): the activity of PITPα increased, whereas that of PITPβ remained unchanged. As compared to donor and acceptor membranes prepared without cholesterol, the addition of cholesterol (χ = 0.47) to Cer*P*Cho membranes resulted in an increase in Cer*P*Cho transfer activity of 3-fold for PITPβ, and the addition of cholesterol (χ = 0.47) to PtdCho membranes resulted in an increase in PtdCho transfer activity of 1.5-fold for PITPα. Lower levels of cholesterol (χ < 0.33) had no effect on PtdCho and Cer*P*Cho transfers catalyzed by either isoform.

To determine if the location of cholesterol in the vesicle populations affected transfer rate enhancement, we prepared donors and acceptors with and without cholesterol. Using these four populations in various combinations, we found that it was the cholesterol associated with the acceptor vesicles that had the greater impact on first-order rates of protein-catalyzed transfer (Figure 2). The most favorable location was cholesterol solely in the acceptor vesicles. Similar results were obtained with PITPα (data not shown). In the remaining experiments to be described, we focused primarily on the effects of acceptor vesicle cholesterol content on phospholipid transfer mediated by PITPβ. It should also be noted that no differences were observed in the current substitution of LacPtdEtn for LacCer (*32*) as the galactose-containing lipid essential for the agglutination and precipitation of donor vesicles during the course of transfer assays.

PITPβ transfers PtdCho and PtdIns between membranes. We measured their transport from bulk PtdCho donors to acceptors prepared from either brain Cer*P*Cho or PtdCho

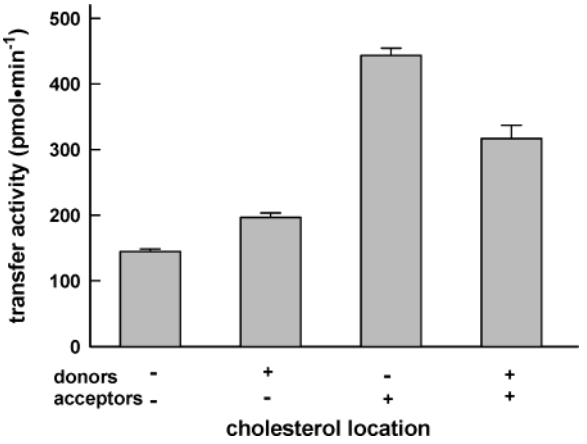

FIGURE 2: Addition of cholesterol to different vesicle populations. Donor and acceptor vesicles were prepared from brain Cer*P*Cho, PtdOH, and LacPtdEtn (88:2:10, mol %) and brain Cer*P*Cho and PtdOH (98:2, mol %), respectively. Cholesterol ($\chi = 0.47$) was added to one or both vesicle populations, as indicated. Cer*P*Cho transfer activity was measured with 4 μg of PITPβ; bar heights represent the mean ± SD of three determinations.

and containing no or near stoichiometric amounts of cholesterol. Complementing what we had observed earlier, lipid transfer to Cer*P*Cho vesicles was enhanced dramatically in the presence of cholesterol, with a 6-fold increase for PtdCho and 2.5-fold increase for PtdIns (Table 1). However, the transfer of PtdIns to PtdCho vesicles, like that of PtdCho to PtdCho vesicles, was insensitive to cholesterol. For the experiments in which Cer*P*Cho acceptors vesicles were used, the movement of PtdIns and PtdCho from donor vesicles represented net transfer of these glycerophospholipids (i.e., a unidirectional influx presumably balanced (though not measured directly) by an equivalent efflux of Cer*P*Cho from acceptor vesicles).

Extent of Lipid Transfer in Absence and Presence of Cholesterol. In our typical assay system, we use a mixture of vesicles such that there are 100 nmol of donors (0.25 mM) and 300 nmol of acceptors (0.75 mM). When the transferred lipid (e.g., Cer*P*Cho) is also the bulk membrane lipid at 88 or 98 mol %, these amounts and compositions generate 88 and 264 nmol, respectively, in the donor and acceptor pools. We determined the fraction of the donor pool that was available for transfer by performing Cer*P*Cho transfer assays in the presence of an excess of PITPβ (Figure 3). As expected, the kinetics of transfer under these conditions were rapid; after 5 min, there was little further change in the amount of lipid transferred. Moreover, inclusion of cholesterol in the acceptor vesicles had no significant effect on the protein-dependent influx of Cer*P*Cho from donor vesicles. The extent of transfer in the early phase (20−25 nmol) was consistent with a population of essentially unilamellar donor vesicles in which the initial distribution of lipid is 23% of the total present in the assay, whose radii are 35−45 nm (Table 3) and whose outer layer contains 55−60% of the lipid (*38*). The increase with time in the approach to equilibrium was most likely attributable to a slow translocation of radiolabeled Cer*P*Cho from the inner to the outer layer of the donor membrane bilayer. In routine lipid transfer measurements, we attempted to maintain first-order relationships between transfer activity and protein throughout the 30 min incubation.

Influence of CerPCho Acyl Composition on Phospholipid Transfer. Vesicles were prepared from several natural and synthetic Cer*P*Cho species to determine if the acyl composition of the interfacial lipid influenced protein-mediated phospholipid transfer and the influence of cholesterol on transfer. We compared four species (brain, egg, 18:1(9), and 14:0), each of which was used in the preparation of both donor and acceptor vesicles for a given set of assays. In all experiments, however, the trace amount of radiolabeled brain Cer*P*Cho in the donor populations was derived from bovine brain. Like brain Cer*P*Cho in earlier experiments, egg Cer*P*Cho supported comparable rates of lipid transfer (Table 2). While the unsaturated 18:1(9)-Cer*P*Cho provided a much more favorable membrane surface for PITPβ interaction and lipid exchange, the shorter, saturated 14:0-Cer*P*Cho was essentially inactive. Incorporation of cholesterol ($\chi = 0.47$) into acceptor vesicles moderately improved PITPβ-catalyzed Cer*P*Cho transfer to brain Cer*P*Cho and 18:1(9)-Cer*P*Cho membranes. A similar level of cholesterol dramatically increased lipid transfer to 14:0-Cer*P*Cho vesicles. In sharp contrast, cholesterol reduced the quality of egg Cer*P*Cho vesicles to function as acceptors. Dihydrocholesterol, a more chemically stable analogue of cholesterol, was also able to enhance transfer activity.

Effect of CerPCho Acyl Composition and Cholesterol on Vesicle Size and Membrane Microviscosity. Concerned that the different lipid compositions used in our transfer studies could result in vesicles of different size, we studied Cer*P*Cho and PtdCho vesicles by dynamic light scattering. Data fitting, using monomodal cumulants analysis, yielded values for the hydrodynamic radius of each vesicle population (Table 3). The observed range of particle size is 35−62 nm, consistent with large unilamellar vesicles and comparable to PtdCho vesicles prepared similarly by ethanol injection (*39*). Inclusion of LacPtdEtn in the donor membranes resulted in somewhat smaller vesicles, while the addition of cholesterol usually promoted a modest increase in vesicle size.

To characterize further the vesicles, we obtained measurements of steady-state fluorescence anisotropy of the lipid-soluble molecule DPH. Anisotropy can, in turn, be used to approximate microviscosity (*36*). As compared to Cer*P*Cho vesicles containing no cholesterol, the inclusion of cholesterol ($\chi = 0.33$ or 0.47) caused a significant increase in membrane microviscosity (Table 3). This increase held for all Cer*P*Cho species examined, both natural and synthetic. Not unexpectedly, donor vesicles that contained the *sn*-1,2-dioleoyl species of LacPtdEtn (10 mol %) were uniformly less viscous than their acceptor vesicle counterparts.

Action of Cholesterol-Binding Agents on Protein-Mediated Phospholipid Transfer. Knowing that the addition of cholesterol to Cer*P*Cho membranes strongly affected the rates of intermembrane phospholipid transfer, we were interested to see if such changes could be reversed. Accordingly, we employed several previously characterized agents that are capable of binding and potentially extracting membrane-associated cholesterol. One class of such agents is the β-CDs, a family of $\alpha(1 \rightarrow 4)$-linked D-glucose cyclical heptamers with a conical frustum shape and relatively hydrophobic cavity (*40*). Having already demonstrated a significant enhancement in Cer*P*Cho transfer activity using vesicles containing cholesterol, we employed acceptor vesicles containing cholesterol ($\chi = 0.47$) and lacking cholesterol as

Table 1: Effect of Acceptor Vesicle Cholesterol Content on Glycerophospholipid Transfer

lipid composition[a]		transfer activity[b] (pmol min^{-1})	
donor vesicles	acceptor vesicles	**PtdCho**	**PtdIns**
PtdCho/PtdOH/LacPtdEtn (88:2:10, mol %)	brain Cer*P*Cho/PtdOH (98:2, mol %)	26.6 ± 5.7	n.d.[c]
PtdCho/PtdOH/LacPtdEtn (88:2:10, mol %)	brain Cer*P*Cho/PtdOH (98:2, mol %) + cholesterol	146.9 ± 3.9	n.d.
PtdCho/**PtdIns**/LacPtdEtn (85:5:10, mol %)	brain Cer*P*Cho/PtdOH (98:2, mol %)	n.d.	2.0 ± 0.2
PtdCho/**PtdIns**/LacPtdEtn (85:5:10, mol %)	brain Cer*P*Cho/PtdOH (98:2, mol %) + cholesterol	n.d.	5.1 ± 0.3
PtdCho/**PtdIns**/LacPtdEtn (85:5:10, mol %)	PtdCho/PtdOH (98:2, mol %)	n.d.	29.9 ± 1.2
PtdCho/**PtdIns**/LacPtdEtn (85:5:10, mol %)	PtdCho/PtdOH (98:2, mol %) + cholesterol	n.d.	30.6 ± 0.3

[a] Transferable (radiolabeled) lipids are identified by boldface. Where indicated, acceptor vesicles contain cholesterol ($\chi = 0.47$). [b] Transfer activity is determined at 37 °C for 30 min incubations of 0.25 mM donor vesicles, 0.75 mM acceptor vesicles, and 0.3 μg of PITPβ in a total volume of 0.4 mL. Results from triplicate incubations are calculated for transfer of PtdCho or PtdIns and presented as mean ± SD. [c] n.d., not determined.

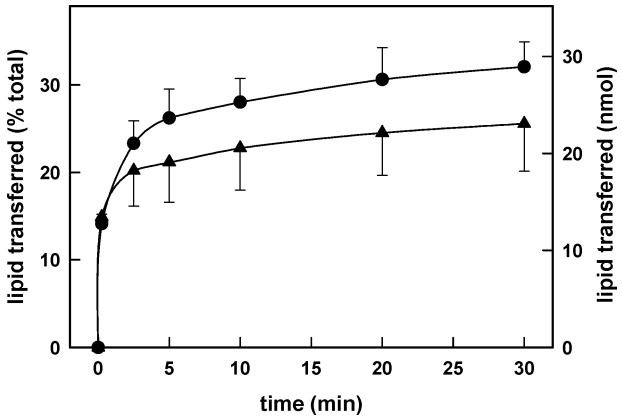

FIGURE 3: Kinetics of lipid transfer with an excess of PITPβ. Donor and acceptor vesicles were prepared from brain Cer*P*Cho, PtdOH, and LacPtdEtn (88:2:10, mol %) and Cer*P*Cho and PtdOH (98:2, mol %), respectively. In the acceptor vesicle population, cholesterol was absent (▲) or present at $\chi = 0.47$ (●). Cer*P*Cho transfer activity was measured with 20 μg of PITPβ. The amount of donor Cer*P*Cho transferred during the 30 min incubation is given as % total (left axis) or nmol (right axis). Data points reflect the mean ± SD of three determinations.

beginning and end reference points, respectively. As the amount of CD added to the system was increased, the magnitude of cholesterol-induced enhancement declined (Figure 4). At concentrations of 1−10 mM, these agents were able to abolish all of the increased activity gained upon inclusion of cholesterol in the acceptors. Transfer activity using vesicles lacking cholesterol but exposed to 0.1 or 1 mM CD differed little from those not exposed to the cholesterol-binding agents (data not shown). However, the more hydrophobic CDs, at concentrations ≥3 mM, interfered with vesicle recoveries and led to artifacts of unusually high blanks and low transfer activities (Figures 4 and 5). Among the unmodified and alkylated CDs tested, the order of effectiveness was Me-β-CD > β-CD > HOPr-β-CD. Filipin, a polyene macrolide isolated from *Streptomyces filipinensis*, also has cholesterol sequestering properties. At a concentration of 125 μg mL^{-1} (0.2 mM), filipin led to a complete reversal of cholesterol-induced transfer enhancement (data not shown); however, a poor recovery of acceptor vesicles precluded its further utility in our experiments.

Specificity and Time Course of Cyclodextrin Treatment. In initial experiments, we added CDs to our complete assay system, such that their exposure to cholesterol-containing vesicles was only 30 min. We compared these conditions with a 60 min incubation in which donor vesicles were or were not present and PITPβ was absent. Thereafter, missing assay components were added, and the usual incubation was conducted. In the absence of donor vesicles, the additional 60 min incubation provided no change in transfer activity for β-CD or HOPr-β-CD when used at 3 mM (Figure 5A). However, with the inclusion of donor vesicles during this 60 min incubation, a significant reversal of cholesterol enhancement was noted. Using β-CD at 3 mM in the presence of donor vesicles, a more detailed time course was examined. Beyond 60 min of exposure, there was no further decline in Cer*P*Cho transfer activity (Figure 5B), suggesting that whatever proportion of cholesterol had been sequestered in or deleted from the acceptor vesicles was sufficient to mimic conditions in which no cholesterol was present.

Binding of PITPβ to Vesicles Prepared from CerPCho and Cholesterol. Molecular sieve chromatography has proven useful in monitoring the interaction of native PITPα and truncated derivatives with anionic phospholipid vesicles (*37*). These earlier data suggested that as the proportion of protein that bound tightly to vesicles increased, the transfer activity decreased. We, therefore, carried out a similar analysis of PITPα and PITPβ to ascertain whether differences in transfer rate with cholesterol-poor and cholesterol-rich Cer*P*Cho membranes correlated with the protein's affinity for these vesicles. Unlike PITPα, chromatography of PITPβ in the absence of vesicles revealed a doublet that eluted at 9−11 min (Figure 6). We currently have no explanation for the complex elution profile of behavior PITPβ. In the presence of vesicles lacking cholesterol, an additional protein peak was noted at 6 min, representing protein strongly associated with the vesicles that are eluted in the column's void volume. In the presence of vesicles containing cholesterol ($\chi = 0.47$), however, the amount of protein eluting in the void volume decreased dramatically. Thus, semiquantitative integration of duplicate profiles of PITPβ yields 5−16% bound to cholesterol-rich acceptor vesicles and 24−27% bound to cholesterol-poor acceptor vesicles. A similar, although less striking, trend was noted for the association of PITPβ with donor vesicles. We infer from these results that PITPβ exhibits a reduced affinity for Cer*P*Cho-cholesterol membranes.

Table 2: Transfer of Cer*P*Cho Using Donor and Acceptor Membranes Composed of Cer*P*Cho Species of Different *N*-Acyl Composition

molecular species of Cer*P*Cho		Cer*P*Cho transfer activity[b] (pmol min^{-1})
donor vesicles	acceptor vesicles[a]	
brain Cer*P*Cho/PtdOH/LacPtdEtn (88:2:10, mol %)	brain Cer*P*Cho/PtdOH (98:2, mol %)	140.1 ± 16.5
brain Cer*P*Cho/PtdOH/LacPtdEtn (88:2:10, mol %)	brain Cer*P*Cho/PtdOH (98:2, mol %) + cholesterol	290.8 ± 52.1
brain Cer*P*Cho/PtdOH/LacPtdEtn (88:2:10, mol %)	brain Cer*P*Cho/PtdOH (98:2, mol %) + dihydrocholesterol	256.0 ± 8.0
egg Cer*P*Cho/PtdOH/LacPtdEtn (88:2:10, mol %)	egg Cer*P*Cho/PtdOH (98:2, mol %)	151.6 ± 37.4
egg Cer*P*Cho/PtdOH/LacPtdEtn (88:2:10, mol %)	egg Cer*P*Cho/PtdOH (98:2, mol %) + cholesterol	21.3 ± 4.8
14:0-Cer*P*Cho/PtdOH/LacPtdEtn (88:2:10, mol %)	14:0-Cer*P*Cho/PtdOH (98:2, mol %)	0.7 ± 0.1
14:0-Cer*P*Cho/PtdOH/LacPtdEtn (88:2:10, mol %)	14:0-Cer*P*Cho/PtdOH (98:2, mol %) + cholesterol	15.8 ± 1.9
18:1(9)-Cer*P*Cho/PtdOH/LacPtdEtn (88:2:10, mol %)	18:1(9)-Cer*P*Cho/PtdOH (98:2, mol %)	283.5 ± 9.3
18:1(9)-Cer*P*Cho/PtdOH/LacPtdEtn (88:2:10, mol %)	18:1(9)-Cer*P*Cho/PtdOH (98:2, mol %) + cholesterol	404.9 ± 2.5

[a] Where indicated, acceptor vesicles contain cholesterol or dihydrocholesterol ($\chi = 0.47$). [b] Transfer activity is determined at 37 °C for 30 min incubations of 0.25 mM donor vesicles, 0.75 mM acceptor vesicles, and 4 μg of PITPβ in a total volume of 0.4 mL. Results are based on the transfer of Cer*P*Cho in three to nine measurements and presented as mean ± SD.

Table 3: Effect of Vesicle Lipid Composition on Hydrodynamic Radius and Membrane Microviscosity

lipid composition		hydrodynamic radius[a] (nm)	fluorescence anisotropy[b]
phospholipids	cholesterol (mole fraction)		
brain Cer*P*Cho/PtdOH/LacPtdEtn (88:2:10, mol %)	0	36.5 ± 3.4	0.144 ± 0.004
	0.47	56.9 ± 2.8	0.186 ± 0.001
brain Cer*P*Cho/PtdOH (98:2, mol %)	0	45.9 ± 3.0	0.187 ± 0.024
	0.33	52.8 ± 1.8	0.235 ± 0.003
	0.47	52.5 ± 1.5	0.252 ± 0.005
egg Cer*P*Cho/PtdOH/LacPtdEtn (88:2:10, mol %)	0	46.8 ± 1.6	0.108 ± 0.005
	0.47	62.4 ± 3.1	0.146 ± 0.002
egg Cer*P*Cho/PtdOH (98:2, mol %)	0	49.2 ± 3.8	0.135 ± 0.010
	0.47	57.8 ± 1.9	0.250 ± 0.008
18:1(9)-Cer*P*Cho/PtdOH/LacPtdEtn (88:2:10, mol %)	0	35.1 ± 1.2	0.070 ± 0.001
	0.47	41.9 ± 1.4	0.179 ± 0.004
18:1(9)-Cer*P*Cho/PtdOH (98:2, mol %)	0	47.5 ± 1.9	0.066 ± 0.002
	0.47	51.5 ± 2.6	0.200 ± 0.001
14:0-Cer*P*Cho/PtdOH (98:2, mol %)	0	49.6 ± 1.4	0.090 ± 0.006
	0.47	52.2 ± 3.4	0.227 ± 0.011

[a] Hydrodynamic radius, determined at 20 °C, is presented as mean ± SD of data collected from a minimum of 20 consecutive measurements of one to three vesicle preparations ($n = 20-60$). [b] Steady-state fluorescence anisotropy of 1,6-diphenyl-1,3,5-hexatriene, measured at 37 °C, is presented as mean ± SD of data collected from three to five measurements of one to three vesicle preparations ($n = 3-13$).

DISCUSSION

Remarkable among the observations presented here are those that underscore the selective nature of cholesterol's ability to influence the activity of protein-mediated intermembrane phospholipid transport. First, and foremost, the β isoform of rat PITP is more sensitive to membrane cholesterol than is the α isoform. Second, a relatively high membrane content of cholesterol ($\chi > 0.4$) is required to elicit increases in the rates of phospholipid transport. These effects are more pronounced when the bulk membrane lipid and the transported lipid are Cer*P*Cho and when the sterol is a component of the acceptor vesicle. Third, treatment of cholesterol-rich membranes with sterol-binding agents shows that PITPβ activity changes are fully reversible. Finally, the mechanism by which cholesterol enhances the activity of PITPβ appears to involve a decreased affinity of the protein for a liquid-ordered membrane surface, in a manner that is independent of vesicle size and membrane microviscosity.

Specific interactions between Cer*P*Cho and cholesterol, described in bilayer and monolayer systems (*41*, *42*), lead to the formation of stoichiometric, liquid-crystalline complexes in which liquid-disordered and -ordered phases coexist. The amount of cholesterol required to form these condensed complexes is in the range of $0.1 < \chi_{cholesterol} < 0.8$; however, at $\chi > 0.3$, the liquid-ordered phase predominates (*41*, *43*). There is general agreement that intermolecular hydrogen bonds play a role in the formation and stabilization of Cer*P*Cho and cholesterol complexes, specifically between the 3β-OH group of the sterol and the amide group of the sphingolipid (*41*, *42*). Indeed, recent electron spin resonance and infrared spectroscopic measurements provide direct evidence for such hydrogen bonds (*44*). In experiments in which we examined a range of membrane cholesterol content, we generally observed a threshold of $\chi = 0.33-0.40$ for any alteration of intermembrane lipid transport catalyzed by PITPβ. This threshold was required for Cer*P*Cho transfer

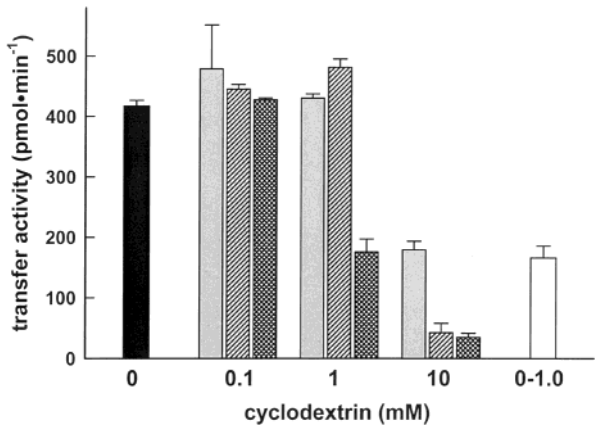

FIGURE 4: Action of cholesterol-binding agents on phospholipid transfer. Donor vesicles consisted of brain Cer*P*Cho, PtdOH, and LacPtdEtn (88:2:10, mol %); acceptor vesicles were prepared from brain Cer*P*Cho and PtdOH (98:2, mol %) and contained cholesterol ($\chi = 0.47$). Prior to the addition of PITP and donor vesicles to the assay system, acceptor vesicles were incubated at 37 °C for 10 min with various CDs at the indicated concentrations: HOPr-β-CD (no pattern); β-CD (diagonal); or Me-β-CD (crosshatch). Cer*P*Cho transfer activity was measured with 4 μg of PITPβ; bar heights represent the mean ± SD of three determinations. Data are also presented for incubations to which no CD was added to acceptor vesicles containing cholesterol (black bar) and CD up to 1.0 mM was added to acceptor vesicles lacking cholesterol (white bar); these data were used as beginning and end reference points, respectively.

between Cer*P*Cho vesicles and PtdIns transfer from PtdCho donor vesicles to Cer*P*Cho acceptor vesicles; activities were 2−6-fold enhanced as compared to those determined at $\chi_{cholesterol} < 0.25$. For other transfer pathways, including PtdCho or PtdIns transfer between PtdCho vesicles, cholesterol-induced enhancements were no more than 1.5-fold or altogether absent. Clearly, our threshold of cholesterol for an influence on PITP-mediated lipid transport is similar to that required for the formation of liquid-ordered phases.

We were able to eliminate several potential factors in the differences observed for lipid transport in the absence and presence of cholesterol. One of these could have been a change in the availability of vesicle Cer*P*Cho for PITPβ. In experiments employing a large excess of PITPβ, we showed that there was no significant difference in either transfer kinetics or the donor−acceptor equilibrium attained (Figure 3). Another factor could have been major differences in the size of the vesicles used in our assays. We found that vesicle radii were generally in the range of 40−55 nm (Table 1), similar to those reported for synthetic PtdCho vesicles prepared by solvent injection (*39*), and only modestly dependent on cholesterol content. Within this spectrum of radii, we anticipate that changes in vesicle curvature would not appreciably influence PITP activity (*45*).

Whatever the molecular basis of cholesterol's ability to modulate the activity of PITPβ, the effects were fully reversible. We took advantage of a wealth of experimental literature on the use of cyclodextrins to facilitate the efflux of cholesterol from natural and model membranes (*43*, *46*−*48*). Treatment of Cer*P*Cho-cholesterol vesicles (donors or acceptors) with cyclodextrins, before their introduction into a transfer assay, gave results that were consistent with the removal of cholesterol and the behavior of the vesicles as if they contained less or no cholesterol (Figures 3−5). The depletion of cholesterol was both time- and dose-dependent. There was also a greater decrease in transfer activity when cholesterol-rich acceptor vesicles were treated with β-CDs in the presence of donor vesicles, suggesting that cholesterol depletion of the acceptor vesicle is accompanied by import into the donor vesicle. Such a mechanism has recently been proposed for a comparable donor−acceptor vesicle system developed to investigate cholesterol partition coefficients (*48*). The efficiency among structurally different β cyclodextrins in our investigations was Me-β-CD > β-CD > HO-Pr-β-CD, similar to that reported in their use in mediating cholesterol efflux from cultured cells or lipid vesicles (*46*, *48*). Consistent with our results was the observation that β-CD extracts cholesterol more rapidly from liquid-ordered surfaces than from liquid-disordered surfaces (*43*).

In monolayer mixtures of cholesterol and Cer*P*Cho, surface pressure and molecular area measurements defined liquid−liquid miscibility critical points (*43*, *49*). These points have been interpreted as the coexistence, at $\chi_{cholesterol} \geq 0.40$, of a liquid-ordered phase of sphingolipid and cholesterol and a liquid cholesterol phase. As the cholesterol component increased relative to the sphingolipid, the molecular area decreased monotonically until $\chi_{cholesterol} = 0.40$, above which the area remained constant. These data described a progressive condensation of the Cer*P*Cho-cholesterol membrane into small, compact domains. The association of PITPβ with similar domains in model membranes is necessarily transient, given the kinetics and molecularity of protein-catalyzed intermembrane phospholipid transport (*33*, *50*). Further, the more productive association must presumably be with the liquid-ordered Cer*P*Cho-cholesterol phase because protein dissociation requires occupancy of the lipid-binding cavity (i.e., a holoprotein), such that equivalent bidirectional fluxes are maintained (*27*, *51*). We propose that the increased efficiency of lipid transfer into/from liquid-ordered domains arises from a more rapid association−dissociation cycle, during which protein−membrane lipid exchange occurs. Decreased affinities of both PITP isoforms for cholesterol-rich surfaces are suggested by molecular sieve separation of free and vesicle-associated protein (Figure 6). Indeed, PITPβ was considerably more sensitive to membrane cholesterol. These data offer an insight into the results presented in Figure 2. Recognizing that a PITPβ is capable of productive transfer paths between any two vesicles and appreciating that our assay is limited to monitoring just one of those (i.e., donor to acceptor), it is likely that the most probable path is the one in which the protein interacts strongly with the vesicle donating a lipid (donor lacking cholesterol) and interacts weakly with the vesicle ultimately accepting that lipid (acceptor containing cholesterol). We may interpret strong and weak interactions in terms of resident time of protein on the vesicle surface, during which protein- and membrane-bound lipids are exchanged: the more protein bound, the longer the resident time.

In the studies described in this paper, we used brain Cer*P*Cho, whose *N*-acyl species include 30% 18:0, 21% 24:1(15), and 13% 24:0, and egg Cer*P*Cho that consists of 85% 16:0 (*52*−*54*). We also employed the synthetic molecules 14:0-Cer*P*Cho and 18:1(9)-Cer*P*Cho. Remarkably, the liquid-disordered/-ordered phase behavior and the average molecular area of binary mixtures of synthetic Cer*P*Cho and cholesterol were essentially independent of the amide-linked

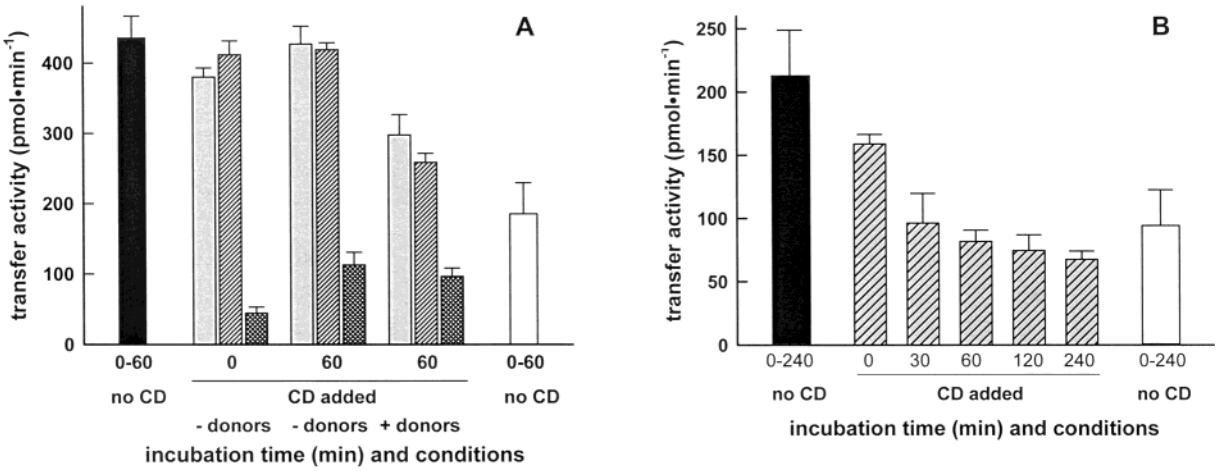

FIGURE 5: Specificity and time course of cyclodextrin treatment. Donor vesicles consisted of brain Cer*P*Cho, PtdOH, and LacPtdEtn (88:2:10, mol %); acceptor vesicles were prepared from brain Cer*P*Cho and PtdOH (98:2, mol %) and contained cholesterol at $\chi = 0.47$. (A) Prior to the addition of PITPβ, acceptor vesicles were incubated at 37 °C for 0 or 60 min with 3 mm CD: HOPr-β-CD (no pattern); β-CD (diagonal); or Me-β-CD (crosshatch). The absence or presence of donor vesicles during this exposure to CD is indicated. Cer*P*Cho transfer activity was measured with 4 μg of PITPβ. (B) Prior to the addition of PITP, donor and acceptor vesicles were incubated at 37 °C for the indicated time with 3 mm β-CD (diagonal). Cer*P*Cho transfer activity was measured with 2 μg of PITPβ. For both sets of experiments, bar heights represent the mean ± SD of three determinations. Data are also presented for incubations to which no CD was added; acceptor vesicles containing cholesterol (black bar) and acceptors lacking cholesterol (white bar) were used as beginning and end reference points, respectively.

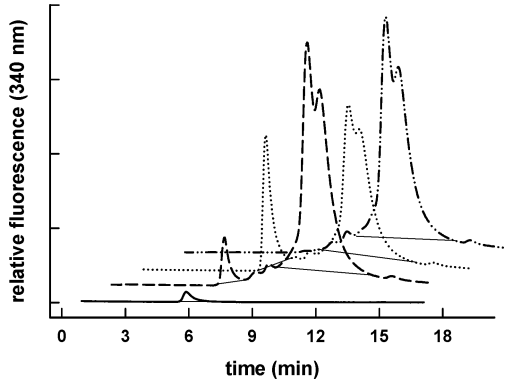

FIGURE 6: Association of PITPβ with phospholipid vesicles. Vesicles were prepared from brain Cer*P*Cho and PtdOH (98:2, mol %) and where indicated cholesterol at $\chi = 0.47$. PITPβ (20 μg) was incubated in 300 μL of assay buffer in the absence or presence of 0.75 mm vesicles at 37 °C for 30 min. From these mixtures, 250 μL aliquots were analyzed by molecular sieve HPLC, as described in the Materials and Methods. Protein was monitored by intrinsic Trp fluorescence, using λ_{ex} of 290 nm and λ_{em} of 340 nm. Elution profiles, offset −2 min, correspond to vesicles containing cholesterol (solid line), PITPβ with vesicles containing cholesterol (dashed line), PITPβ with vesicles lacking cholesterol (dotted line), and PITPβ alone (dashed−dotted line). Peak areas are estimated by isolation of the principal peaks (indicated by thin lines) and manual weighing.

acyl chain length for the series 14:0−26:0-Cer*P*Cho (*55*). Thermal phase transitions of amphipathic lipids, in general, become more muted as the content of cholesterol increases. At $\chi_{cholesterol} \geq 0.30$, there are no enthalpic changes detectable by calorimetry, nor are there significant viscosity changes monitored by steady-state fluorescence polarization (*57*−*59*). In the absence of sterol, the acyl chain-melting transition temperatures for natural and synthetic sphingomyelins fall within a surprisingly narrow range: 36−39 °C for brain and egg Cer*P*Cho; 25−30 °C for 24:1(15)-Cer*P*Cho; and 41−48 °C for the series 16:0−24:0-Cer*P*Cho (*46*, *58*−*60*). From our transfer activity measurements, analyses of steady-state fluorescence anisotropy, and estimations of membrane microviscosity, we are forced to conclude that acyl chain order makes no direct contribution to differences among the various Cer*P*Cho species tested. For acceptor vesicles that contained no cholesterol, brain Cer*P*Cho was the most active; this species was, however, the most viscous. These data contrast sharply with acceptor vesicles that contain cholesterol. Although microviscosity among Cer*P*Cho species was not dissimilar, transfer rates differed widely.

From what our investigations have informed us about preferential interactions of PITPβ with liquid-ordered domains of Cer*P*Cho and cholesterol in model membranes, we can now speculate on possible parallels within cells. Much evidence supports the contention that those sphingolipid- and cholesterol-rich membrane microdomains identified as rafts and caveolae are liquid-ordered in their chemical-physical properties (*21*, *22*, *25*). Indeed, hydrogen bond networks among Cer*P*Cho and cholesterol molecules and interdigitations of acyl chains within the bilayer not only stabilize liquid-ordered domains in model membranes but are largely responsible for the detergent insolubility of rafts in natural membranes. Accessibility of intracellular PITPβ to Cer*P*Cho- and cholesterol-rich membranes may be limited. Although Cer*P*Cho and cholesterol are predominately sorted to the plasma membrane (*20*, *24*, *25*), their topological distribution across that membrane differs. Cer*P*Cho appears to be −80% localized on the exoplasmic surface (*61*, *62*); in contrast, cholesterol is more equally divided between the exoplasmic and the cytosolic surfaces (*63*). While the portion of Cer*P*Cho on the cytosolic surface of the plasma membrane is small, it nevertheless is associated with a highly cholesterol-enriched environment. Indeed, it is most likely that this microdomain pool of Cer*P*Cho participates in signal transduction and apoptosis (*64*, *65*) and is a substrate for PITPβ-mediated (intermembrane) transport.

The principal protein components of caveolar microdomains are the caveolins, palmitoylated membrane proteins that form oligomers and bind cytosolic proteins (*66*). The attraction of other proteins to caveolin is through the caveolin

scaffolding domain, whose target consensus-binding motifs are rich in aromatic amino acids. Mammalian PITPβ, but significantly not PITPα, contains one of these motifs: FHEKAWNAY [ΦXXXXΦXXΦ, where Φ is F, W, or Y] at residues 83−91. Although this sequence is part of one of the β strands that comprises the lipid-binding cavity, the homologous residues in the tertiary structure of PITPα exhibit considerable exposure on the protein's surface (*6*). It is, therefore, not unreasonable to anticipate in vivo specific interactions between PITPβ and caveolins to promote localized changes in lipid metabolism and/or membrane composition.

In summary, our studies are consistent with the possibility that PITPβ exhibits a preference for a liquid-ordered phase formed by Cer*P*Cho and cholesterol and that these transient surface interactions result in enhanced rates of intermembrane lipid transport. We also envisage directed associations within the cell between PITPβ and membrane microdomains such as rafts and caveolae. Yet to be defined are the molecular details of the interfacial complex between PITPβ and membrane. Several experimental approaches are being pursued, including site-specific mutagenesis, dynamic fluorescence and circular dichroism spectroscopy, and structural determination of membrane-associated PITPβ.

ACKNOWLEDGMENT

We sincerely acknowledge the generosity of Prof. K. Hosaka (Department of Basic Sciences for Medicine, School of Health Sciences, Gunma University, Maebashi 371-8514, Japan) for the gift of a full-length cDNA encoding rat PITPβ and that of Prof. R. E. Brown (Section of Membrane Biochemistry, The Hormel Institute, University of Minnesota, Austin, MN) for the gift of *N*-myristoyl-sphingomyelin. We thank Prof. M. D. Yoder (Division of Cell Biology and Biophysics, School of Biological Sciences, University of Missouri−Kansas City, Kansas City, MO) for access to dynamic light scattering instrumentation. We are most grateful to J. M. Tremblay and Prof. L. R. Yarbrough (Department of Biochemistry and Molecular Biology, University of Kansas Medical Center) for some of the protein used in the current studies and helpful discussions during the preparation of this manuscript.

REFERENCES

1. Wirtz, K. W. A., and Zilversmit, D. B. (1968) Exchange of phospholipids between liver mitochondria and microsomes in vitro, *J. Biol. Chem. 243*, 3596−3602.
2. Kamp, H. H., Wirtz, K. W. A., and van Deenen, L. L. M. (1973) Some properties of phosphatidylcholine exchange protein purified from beef liver, *Biochim. Biophys. Acta 318*, 313−325.
3. Helmkamp, G. M., Jr., Harvey, M. S., Wirtz, K. W. A., and van Deenen, L. L. M. (1974) Phospholipid exchange between membranes: purification of bovine brain proteins that preferentially catalyze the transfer of phosphatidylinositol, *J. Biol. Chem. 249*, 6382−6389.
4. DiCorleto, P. E., Warach, J. B., and Zilversmit, D. B. (1979) Purification and characterization of two phospholipid exchange proteins from bovine heart, *J. Biol. Chem. 254*, 7795−7802.
5. Tsujishata, Y., and Hurley J. H. (2000) Structure and lipid transport mechanism of a StAR-related domain, *Nat. Struct. Biol. 7*, 408−414.
6. Yoder, M. D., Thomas, L. M., Tremblay, J. M., Oliver, R. L., Yarbrough, L. R., and Helmkamp, G. M., Jr. (2001) Structure of a multifunctional protein: Mammalian phosphatidylinositol transfer protein complexed with phosphatidylcholine, *J. Biol. Chem. 276*, 9246−9252.
7. Romanowski, M. J., Soccio, R. E., Breslow, J. L., and Burley, S. K. (2002) Crystal structure of the Mus musculus cholesterol-regulated START protein 4 (StarD4) containing a StAR-related lipid transfer domain, *Proc. Natl. Acad. Sci. U.S.A. 99*, 6949−6954.
8. Roderick, S. L., Chan, W. W., Agate, D. S., Olsen, L. R., Vetting, M. W., Rajashankar, K. R., and Cohen, D. E. (2002) Structure of human phosphatidylcholine transfer protein in complex with its ligand, *Nat. Struct. Biol. 9*, 507−511.
9. Allen-Baume, V., Ségui, B., and Cockcroft, S. (2002) Current thoughts on the phosphatidylinositol transfer protein family, *FEBS Lett. 531*, 74−80.
10. de Vries, K. J., Westerman, J., Bastiaens, P. I. H., Jovin, T. M., Wirtz, K. W. A., and Snoek, G. T. (1996) Fluorescently labeled phosphatidylinositol transfer protein isoforms (α and β), microinjected into fetal bovine heart endothelial cells, are targeted to distinct intracellular sites, *Exp. Cell Res. 227*, 33−39.
11. Li, H., Tremblay, J. M., Yarbrough, L. R., and Helmkamp, G. M., Jr. (2002) Both isoforms of mammalian phosphatidylinositol transfer protein are capable of binding and transporting sphingomyelin, *Biochim. Biophys. Acta 1580*, 67−76.
12. Ségui, B., Allen-Baume, V., and Cockcroft, S. (2002) Phosphatidylinositol transfer protein β displays minimal sphingomyelin transfer activity and is not required for biosynthesis and trafficking of sphingomyelin, *Biochem. J. 366*, 23−34.
13. Stocco, D. M. (2001) StAR protein and the regulation of steroid hormone biosynthesis, *Annu. Rev. Physiol. 63*, 193−213.
14. Klenchin, V. A., and Martin, T. F. J. (2000) Priming in exocytosis, attaining fusion-competence after vesicle docking, *Biochimie 82*, 399−407.
15. Cockcroft, S. (2001) Phosphatidylinositol transfer proteins couple lipid transport to phosphoinositide synthesis, *Semin. Cell Dev. Biol. 12*, 183−191.
16. van Tiel, C. M., Schouten, A., Snoek, G. T., Gros, P., and Wirtz, K. W. A. (2002) The structure of phosphatidylinositol transfer protein α reveals sites for phospholipid binding and membrane association with major implications for its function, *FEBS Lett. 531*, 69−73.
17. de Brouwer, A. P. M., Westerman, J., Kleinnijenhuis, A., Bevers, L. E., Roelofsen, B., and Wirtz, K. W. A. (2002) Clofibrate-induced relocation of phosphatidylcholine transfer protein to mitochondria in endothelial cells, *Exp. Cell Res. 274*, 100−111.
18. Holthuis, J. C. M., Pomorski, T., Raggers, R. J., Sprong, H., and van Meer, G. (2001) The organizing potential of sphingolipids in intracellular membrane transport, *Physiol. Rev. 81*, 1689−1723.
19. Aï t Slimane, T., and Hoekstra, D. (2002) Sphingolipid trafficking and protein sorting in epithelial cells, *FEBS Lett. 529*, 54−59.
20. Zhang, P., Liu, B., Jenkins, G. M., Hannun, Y. A., and Obeid, L. M. (1997) Expression of neutral sphingomyelinase identifies a distinct pool of sphingomyelin involved in apoptosis, *J. Biol. Chem. 272*, 9609−9612.
21. Brown, D. A., and London, E. (2000) Structure and function of sphingolipid- and cholesterol-rich membrane rafts, *J. Biol. Chem. 275*, 17221−17224.
22. van Meer, G., and Lisman, Q. (2002) Sphingolipid transport: rafts and translocators, *J. Biol. Chem. 277*, 25855−25858.
23. Wattenberg, B. W., and Silbert, D. F. (1983) Sterol partitioning among intracellular membranes. Testing a model for cellular sterol distribution, *J. Biol. Chem. 258*, 2284−2289.
24. Lange, Y., Swaisgood, M. H., Ramos, B. V., and Steck, T. L. (1989) Plasma membranes contain half the phospholipid and 90% of the cholesterol and sphingomyelin in cultured human fibroblasts, *J. Biol. Chem. 264*, 3786−3793.
25. Pike, L. J. (2003) Lipid rafts: bringing order to chaos, *J. Lipid Res. 44*, 655−667.
26. Mattjus, P., and Slotte, J. P. (1996) Does cholesterol discriminate between sphingomyelin and phosphatidylcholine in mixed monolayers containing both phospholipids? *Chem. Phys. Lipids 81*, 69−80.
27. Kasper, A. M., and Helmkamp, G. M., Jr. (1981) Intermembrane phospholipid fluxes catalyzed by bovine brain phospholipid exchange protein, *Biochim. Biophys. Acta 664*, 22−32.
28. Dickeson, S. K., Lim, C. N., Schuyler, G. T., Dalton, T. P., Helmkamp, G. M., Jr., and Yarbrough, L. R. (1989) Isolation and sequence of cDNA clones encoding rat phosphatidylinositol transfer protein, *J. Biol. Chem. 264*, 16557−16564.
29. Cawley, D. B., Hedblom, M. L., and Houston, L. L. (1978) Homology between ricin and *Ricinus communis* agglutinin: amino

terminal sequence analysis and protein synthesis inhibition studies, *Arch. Biochem. Biophys. 190*, 744−755.
30. Tremblay, J. M., Helmkamp, G. M., Jr., and Yarbrough, L. R. (1996) Limited proteolysis of rat phosphatidylinositol transfer protein by trypsin cleaves the C terminus, enhances binding to lipid vesicles, and reduces phospholipid transfer activity, *J. Biol. Chem. 271*, 21075−21080.
31. Voziyan, P. A., Tremblay, J. M., Yarbrough, L. R., and Helmkamp, G. M., Jr. (1996) Truncations of the C terminus have different effects on the conformation and activity of phosphatidylinositol transfer protein, *Biochemistry 35*, 12526−12531.
32. Kasper, A. M., and Helmkamp, G. M., Jr. (1981) Protein-catalyzed phospholipid exchange between gel and liquid-crystalline phospholipid vesicles, *Biochemistry 20*, 146−151.
33. Yoshimura, T., Welti, R., and Helmkamp, G. M., Jr. (1988) General kinetic model for protein-mediated phospholipid transfer between membranes, *Arch. Biochem. Biophys. 266*, 299−312.
34. van Paridon, P. A., Gadella, T. W. J., Jr., Somerharju, P. J., and Wirtz, K. W. A. (1988) Properties of the binding sites for the sn-1 and sn-2 acyl chains on the phosphatidylinositol transfer protein from bovine brain, *Biochemistry 27*, 6208−6214.
35. de Brouwer, A. P. M., Versluis, C., Westerman, J., Roelofson, B., Heck, A. J. R., and Wirtz, K. W. A. (2002) Determination of the stability of the noncovalent phospholipid transfer protein−lipid complex by electrospray time-of-flight mass spectrometry, *Biochemistry 41*, 8013−8018.
36. Shinitzky, M., and Barenholz, Y. (1978) Fluidity parameters of lipid regions determined by fluorescence polarization, *Biochim. Biophys. Acta 515*, 367−394.
37. Tremblay, J. M., Voziyan, P. A., Helmkamp, G. M., Jr., and Yarbrough, L. R. (1998) The C terminus of phosphatidylinositol transfer protein modulates membrane interactions and transfer activity but not phospholipid binding, *Biochim. Biophys. Acta 1389*, 91−100.
38. Cullis, P. R, and Hope, M. J. (1991) Physical properties and functional roles of lipids in membranes, in *Biochemistry of Lipids, Lipoproteins and Membranes* (Vance, D. E., and Vance, J. E., Eds.) pp 1−41, Elsevier, Amsterdam.
39. Kremer, J. M. H., van den Esker, M. W. J., Pathmamanoharan, C., and Wiersema, P. H. (1977) Vesicles of variable diameter prepared by a modified injection method, *Biochemistry 16*, 3932−3935.
40. Uekama, K., Hirayama, F., and Irie, T. (1998) Cyclodextrin drug carrier systems, *Chem. Rev. 98*, 2045−2076.
41. Sankaram, M. B., and Thompson, T. E. (1990) Interaction of cholesterol with various glycerophospholipids and sphingomyelin, *Biochemistry 29*, 10670−10675.
42. Bittman, R., Kasireddy, C. R., Mattjus, P., and Slotte, J. P. (1994) Interaction of cholesterol with sphingomyelin in monolayers and vesicles, *Biochemistry 33*, 11776−11781.
43. Radhakrishnan, A., and McConnell, H. M. (2000) Chemical activity of cholesterol in membranes, *Biochemistry 39*, 8119−8124.
44. Veiga, M. P., Arrondo, J. L. R., Goñi, F. M., Alonso, A., and Marsh, D. (2001) Interaction of cholesterol with sphingomyelin in mixed membranes containing phosphatidylcholine, studied by spin-label ESR and IR spectroscopies. A possible stabilization of gel-phase sphingolipid domains by cholesterol, *Biochemistry 40*, 2614−2622.
45. Komatsu, H., Bouma, B., Wirtz, K. W. A., Taraschi, T. F., and Janes, N. (2000) Activity of phosphatidylinositol transfer protein is sensitive to ethanol and membrane curvature, *Biochem. J. 348*, 667−673.
46. Kilsdonk, E. P. C., Yancey, P. G., Stoudt, G. W., Bangeter, F. W., Johnson, W. J., Phillips, M. C., and Rothblat, G. H. (1995) Cellular cholesterol efflux mediated by cyclodextrins, *J. Biol. Chem. 270*, 17250−17256.
47. Ilangumaran, S., and Hoessli, D. C. (1998) Effects of cholesterol depletion by cyclodextrin on the sphingolipid microdomains of the plasma membrane, *Biochem. J. 335*, 433−440.
48. Leventis, R., and Silvius, J. R. (2001) Use of cyclodextrins to monitor transbilayer movement and differential lipid affinities of cholesterol, *Biophys. J. 81*, 2257−2267.
49. Radhakrishnan, A., and McConnell, H. M. (1999) Condensed complexes of cholesterol and phospholipids, *Biophys. J. 77*, 1507−1517.
50. Helmkamp, G. M., Jr., Wirtz, K. W. A., and van Deenen, L. L. M. (1976) Phosphatidylinositol exchange protein: effects of membrane structure and evidence for a ping-pong mechanism, *Arch. Biochem. Biophys. 174*, 592−602.
51. Demel, R. A., Kalsbeek, R., Wirtz, K. W. A., and van Deenen, L. L. M. (1977) The protein-mediated net transfer of phosphatidylinositol in model systems, *Biochim. Biophys. Acta 466*, 10−22.
52. Pullarat, R. K., and Reha, H. (1976) Distribution of positional isomers of monoenoic fatty acids in pig-brain white matter sphingomyelin, *J. Neurochem. 27*, 321−322.
53. Calhoun, W. L., and Shipley, G. G. (1979) Fatty acid composition and thermal behavior of natural sphingomyelins, *Biochim. Biophys. Acta 555*, 436−441.
54. Do, U. H., and Ramachandran, S. (1980) Mild alkali-stable phospholipids in chicken egg yolks: characterization of 1-alkenyl and 1-alkyl-*sn*-glycero-3-phosphoethanolamine, sphingomyelin, and 1-alkyl-*sn*-glycero-3-phosphocholine, *J. Lipid Res. 21*, 888−894.
55. Radhakrishnan, A., Li, X.-M., Brown, R. E., and McConnell, H. M. (2001) Stoichiometry of cholesterol-sphingomyelin condensed complexes in monolayers, *Biochim. Biophys. Acta 1511*, 1−6.
56. Estep, T. N., Mountcastle, D. B., Barenholz, Y., Biltonen, R. L., and Thompson, T. E. (1979) Thermal behavior of synthetic sphingomyelin-cholesterol dispersions, *Biochemistry 18*, 2112−2117.
57. Maulik, P. R., and Shipley, G. G. (1996) *N*-Palmitoyl sphingomyelin bilayers: structure and interactions with cholesterol and dipalmitoylphosphatidylcholine, *Biochemistry 35*, 8025−8034.
58. Massey, J. B. (2001) Interaction of ceramides with phosphatidylcholine, sphingomyelin, and sphingomyelin/cholesterol bilayers, *Biochim. Biophys. Acta 1510*, 167−184.
59. Veiga, M. P., Goñi, F. M., Alonso, A., and Marsh, D. (2000) Mixed membranes of sphingolipids and glycerolipids as studied by spin-label ESR spectroscopy, A search for domain formation, *Biochemistry 39*, 9876−9883.
60. Liu, P., Rudick, M., and Anderson, R. G. W. (2002) Multiple functions of caveolin-1, *J. Biol. Chem. 277*, 41295−41298.
61. Allan, D., and Quinn, P. (1988) Resynthesis of sphingomyelin from plasma membrane phosphatidylcholine in BHK cells treated with *Staphylococcus aureus* sphingomyelinase, *Biochem. J. 254*, 765−771.
62. van Meer, G., and Holthuis, J. C. M. (2000) Sphingolipid transport in eukaryotic cells, *Biochim. Biophys. Acta 1486*, 145−170.
63. Lange, Y., and Slayton, J. M. (1982) Interaction of cholesterol and lysophosphatidylcholine in determining red cell shape, *J. Lipid Res. 23*, 1121−1127.
64. Veldman, R. J., Maestre, N., Aduib, O. M., Medin, J. A., Salvayre, R., and Levade, T. (2001) A neutral sphingomyelinase resides in sphingolipid-enriched microdomains and is inhibited by the caveolin-scaffolding domain: potential implications in tumor necrosis factor signaling, *Biochem. J. 355*, 859−868.
65. Hannun, Y., and Obeid, L. M. (2002) The ceramide-centric universe of lipid-mediated cell regulation: stress encounters of the lipid kind, *J. Biol. Chem. 277*, 25847−25850.
66. Razani, B., Schlegel, A., and Lisanti, M. P. (2000) Caveolin proteins in signaling, oncogenic transformation, and muscular dystrophy, *J. Cell Sci. 113*, 2103−2109.

BI034616N